Shape coexistence in ^{66}Se

Z Elekes, V Panin, T.R Rodríguez, K Sieja, D.S Ahn, A Al-Adili, H Baba, A.I Stefanescu, K.J Cook, Cs Dósa, et al.

Physics Letters B 844 (2023) 138072

Contents lists available at ScienceDirect

Physics Letters B

journal homepage: www.elsevier.com/locate/physletb

Shape coexistence in ^{66}Se

Z. Elekes [a,b,*], V. Panin [c,d], T.R. Rodríguez [e], K. Sieja [f,g], D.S. Ahn [h,o], A. Al-Adili [i], H. Baba [h], A.I. Stefanescu [j], K.J. Cook [k,1], Cs. Dósa [a], N. Fukuda [h], J. Gao [h,l], J. Gibelin [m], K.I. Hahn [n,o], Z. Halász [a], S.W. Huang [h,l], T. Isobe [h], M.M. Juhász [a,b], D. Kim [h,n,o], T. Kobayashi [p], Y. Kondo [k], Z. Korkulu [o,h], A. Kurihara [k], I. Kuti [a], H. Miki [k], K. Miki [p], T. Motobayashi [h], H. Otsu [h], A. Saastamoinen [q], M. Sasano [h], H. Sato [h], T. Shimada [k], Y. Shimizu [h], L.G. Sobotka [r], I. Stefanescu [j,s], L. Stuhl [o,h,a], H. Suzuki [h], H. Takeda [h], Y. Togano [t,h], T. Tomai [k], L. Trache [j], D. Tudor [j,s], T. Uesaka [h], Y. Utsuki [p], H. Wang [k], A. Yasuda [k], K. Yoneda [h], Y. Yoshitome [k]

[a] *Atomki, P.O. Box 51, H-4001 Debrecen, Hungary*
[b] *Institute of Physics, Faculty of Science and Technology, University of Debrecen, Egyetem tér 1., H-4032 Debrecen, Hungary*
[c] *Institut für Kernphysik, Technische Universität Darmstadt, 64289 Darmstadt, Germany*
[d] *GSI Helmoltzzentrum für Schwerionenforschung GmbH, 64291 Darmstadt, Germany*
[e] *Complutense University of Madrid, Avda. de Séneca, 2 Ciudad Universitaria, 28040 Madrid, Spain*
[f] *Université de Strasbourg, IPHC, 23 rue du Loess, 67037 Strasbourg, France*
[g] *CNRS, UMR7178, 67037 Strasbourg, France*
[h] *RIKEN Nishina Center, 2-1 Hirosawa, Wako, Saitama 351-0198, Japan*
[i] *Uppsala University, P.O. Box 256, SE-751 05 Uppsala, Sweden*
[j] *IFIN-HH, Department of Nuclear Physics, Reactorului 30, Măgurele, Romania*
[k] *Department of Physics, Tokyo Institute of Technology, 2-12-1 O-Okayama, Meguro, Tokyo, 152-8551, Japan*
[l] *State Key Laboratory of Nuclear Physics and Technology, School of Physics, Peking University, No. 5 Yiheyuan Road, Haidian district, 100871, Beijing, China*
[m] *LPC Caen, ENSICAEN, Université de Caen, CNRS/IN2P3, F-14050 Caen, France*
[n] *Ewha Womans University, Seoul 120-750, Korea*
[o] *Center for Exotic Nuclear Studies, Institute for Basic Science, Daejeon 34126, Korea*
[p] *Department of Physics, Tohoku University, Sendai 980-8578, Japan*
[q] *Texas A&M University, Department of Physics and Astronomy, 578 University Drive College Station, TX 77843-4242, USA*
[r] *Department of Chemistry, Washington University, One Brookings Drive, St. Louis, MO 63130, USA*
[s] *Doctoral School of Physics, University of Bucharest, 405 Atomiştilor Street, Măgurele, Ilfov, 077125, Romania*
[t] *Department of Physics, Rikkyo University, 3-34-1 Nishi-Ikebukuro, Toshima, Tokyo 172-8501, Japan*

ARTICLE INFO

Article history:
Received 12 April 2023
Received in revised form 21 June 2023
Accepted 5 July 2023
Available online 11 July 2023
Editor: D.F. Geesaman

Keywords:
Neutron knock-out reaction
γ-ray spectroscopy
Nuclear structure
Shape coexistence

ABSTRACT

The nuclear structure of ^{66}Se, nucleus beyond the $N=Z$ line on the proton-rich side of the valley of stability, was investigated by the neutron knock-out reaction ^{67}Se(^{12}C,X)^{66}Se using a ^{12}C target. The analysis of the singles spectrum of the γ-rays emitted during the de-excitation of the populated low-lying excited states revealed two previously detected (927(4) keV, 1460(32) keV) and three new (744(6) keV, 1210(17) keV, 1661(23) keV) transitions. The 744-keV, the 1210-keV, and the 1460-keV transitions were found to be in coincidence with the one at 927 keV. The spectrum coincident with the 927-keV transition showed a further possible transition at 299(35) keV, which was obscured by significant atomic background in the singles spectrum. This transition might correspond to a peak previously reported at 273(5) keV that could not be assigned to ^{66}Se unambiguously. Based on a comparison of the experimental data to theoretical calculations, four new excited states are proposed which suggest that ^{66}Se exhibits shape coexistence.

* Corresponding author at: Atomki, P.O. Box 51, H-4001 Debrecen, Hungary.
E-mail address: elekes@atomki.hu (Z. Elekes).

[1] Present address: Department of Nuclear Physics and Accelerator Applications, Research School of Physics, The Australian National University, Canberra, ACT 2600, Australia.

https://doi.org/10.1016/j.physletb.2023.138072

1. Introduction

The term *shape coexistence* is usually used in nuclear physics to describe the phenomenon that distinct collective properties (e.g., states or bands of states) of a single nucleus appear at low excitation energy in a narrow energy range, which can be associated with different intrinsic shapes [1]. Since the first experimental hints on shape coexistence [2] several decades have passed, and, as a consequence of growing data, this peculiarity has become an ordinary attribute of the nuclear landscape (see e.g., recent reviews [3,4]). The neutron-deficient region extending from the line of stability to the proton dripline bounded by germanium and zirconium isotopes was targeted by many experiments and proved to be a rich ground of important results for shape coexistence (see [4] and references therein).

In particular for selenium isotopes, low-lying 0_2^+ states in ^{72,74,76}Se were firmly established [5–9] while tentatively proposed in ^{70}Se [10]. A recent neutron inelastic scattering experiment on ^{76}Se [11] confirmed coexisting spherical and γ-soft structures, while β-decay studies on ^{72,74}Se [8,12] revealed coexisting near-spherical and prolate bands in these selenium isotopes. Lifetime measurements of the ground state bands in ^{70,72}Se [13] and fusion-evaporation experiments [6,14] at high-spin also suggested such shape coexistence for both nuclei. Furthermore, an intriguing shape change between the mirror-nuclei ^{70}Se (oblate) and ^{70}Kr (prolate) was observed recently [15]. Reaching to the $N = Z$ line, two distinct bands (built on 0_1^+ and 2_2^+) were discovered in ^{68}Se. The properties of these bands were found to be consistent with collective oblate (for the 0_1^+ band) and prolate (for the 2_2^+ band) rotations.

Moving towards the dripline data are scarce. A γ-ray spectroscopic study of ^{66}Se found a low-energy transition assigned to the decay of the first 2^+ state [16], and two additional transitions were discovered using $\beta - \gamma$ tagging of fusion-evaporation recoils, tentatively establishing the ground state band $0_1^+ - 2_1^+ - 4_1^+ - 6_1^+$ [17]. In an effort to investigate if shape coexistence exists in this mass region between the $N = Z$ and driplines, the neutron knock-out reaction from ^{67}Se was used to populate the low-lying states in ^{66}Se and to uncover transitions between them by γ-ray spectroscopy.

2. Experiment

The experiment was performed at the Radioactive Isotope Beam Factory operated by the RIKEN Nishina Center and by the Center for Nuclear Study of the University of Tokyo. A stable primary beam of ^{78}Kr ions at an energy of 345 MeV/u and at an intensity of 400 pnA hit a 2-mm-thick ^{9}Be production target placed at the entrance of the BigRIPS separator [18]. A detailed description of the separator and the identification methods was given earlier [19] thus we recall here only some important points. The radioactive nuclei were formed by the fragmentation process, and the ions of interest were selected by the $B\rho - \Delta E - TOF$ method ($B\rho$: magnetic rigidity, ΔE: energy loss, *TOF*: time of flight) [20] using slits and an aluminum wedged degrader at the first focal plane F1, located between the two dipole magnets D1 and D2 of BigRIPS. During the tuning with reduced primary beam intensity (40 pnA), the isotopes in the radioactive cocktail beam were identified between the focal planes F3 and F7 by time-of-flight, energy-loss, and magnetic-rigidity measurements. Plastic scintillators at F3 and F7 were used to determine the *TOF*, while ΔE was measured by a gas ionization chamber at F7 [21]. Several sets of parallel plate avalanche counters (PPAC) at F3, F5, and F7 [22,23] were applied to monitor the trajectory of the particles. For the high-intensity runs, the BigRIPS settings were left unchanged, and the ionization chamber was removed because it could not handle such a high rate. However, the separation of ^{67}Se ions from the other constituents was completely ensured by the information from the *TOF* and $B\rho$ with a 7.5σ in A/Q. The secondary beam was transported downstream of the focal plane F13 to a 2-mm-thick ^{12}C target where the excited states of ^{66}Se were populated via the neutron knock-out reaction.

The prompt γ rays were detected by the CATANA array [24] consisting of 100 CsI(Na) scintillator crystals packed in five cylindrical layers of 20 units each around the carbon target. This arrangement provided coverage of polar angles between 38° and 90°. The detectors in the array were calibrated for energy using ^{22}Na, ^{60}Co, ^{137}Cs and ^{152}Eu radioactive sources with peak energies of 344.3 keV, 661.7 keV, 778.9 keV, 964.1 keV, 1112.1 keV, 1173.2 keV, 1274.5 keV, 1332.5 keV and 1408.0 keV. The linearity of the detectors found to be excellent with linear correlation coefficient R^2 smaller than 0.9995. The beam-like fragments leaving the target were analyzed by the SAMURAI spectrometer [25] based on $B\rho$, ΔE, and *TOF* measurements. The $B\rho$ values were derived via trajectory determination by multiwire drift chambers located upstream (FDC0, FDC1) and downstream (FDC2, FDC3) of the magnet operated at a central magnetic field of 1.56 T, using the multidimensional fit procedure of the ROOT framework [26]. Downstream of the FDC3 a plastic scintillator wall consisting of 7 bars yielded the ΔE and the *TOF* relative to a plastic detector at F13. The ΔE and the trajectory of the beam-like fragments downstream of the target and upstream of the magnet were also monitored by two pairs of strip silicon detectors placed about 30 cm from each other while the distance between the first pair and the target was 60 cm [27–29]. The pairs consisted of identical units with sensitive areal dimensions of 87.6×87.6 mm^2, thicknesses of 325 µm, and readout-pitch sizes of 684 µm. For the determination of the hit positions x and y, the second units in the pairs were rotated by 90° with respect to the first ones. The unambiguous identification of ^{66}Se fragments was ensured by the obtained 4.1σ separation in Z and 3.2σ separation in A/Q. The total beam intensity was approximately 10^4 particle/s, and 10^3particle/s ^{67}Se ions hit the carbon target every second. The kinetic energy of the ^{67}Se particles was around 250 MeV/u at the entrance of the target and the energy loss amounted to about 80 MeV/u while passing through the carbon sheet. 29000 events associated with detected γ rays were counted in the neutron knock-out reaction channel.

3. Results

Radioactive sources of ^{22}Na, ^{60}Co, ^{137}Cs, and ^{152}Eu were used to calibrate the CATANA detectors for energy. A low-energy-detection threshold of 100 keV was achieved in the laboratory system. The photopeak efficiency of the CATANA array was increased by merging the hits in the adjacent units (<10 cm) originating from a single γ ray undergoing Compton-scattering and/or pair production. The energy of the γ rays emitted by the fast-moving ions was Doppler-corrected using the position information of the detectors relative to the carbon target and the velocity of the ions in the middle of the target. In the Doppler-corrected energy range of 500-1500 keV, the FWHM resolution and the addback efficiency of the array were around 13% and 15%, respectively.

Fig. 1 shows the Doppler-corrected singles spectrum for ^{66}Se from the ^{67}Se(^{12}C,X)^{66}Se reaction channel. It includes a background coming from two components: the low-energy part can be connected to atomic processes, and the high-energy part arises from other sources mainly the reactions of the scattered particles on the materials surrounding the target [30,31]. This composite background was modeled by a double-exponential function with four free parameters which proved to be successful in earlier experiments with a similar scintillator array (e.g., [32–35]). The spectrum clearly shows two strong peaks between 700 keV and 1000 keV, and some other candidates in the range

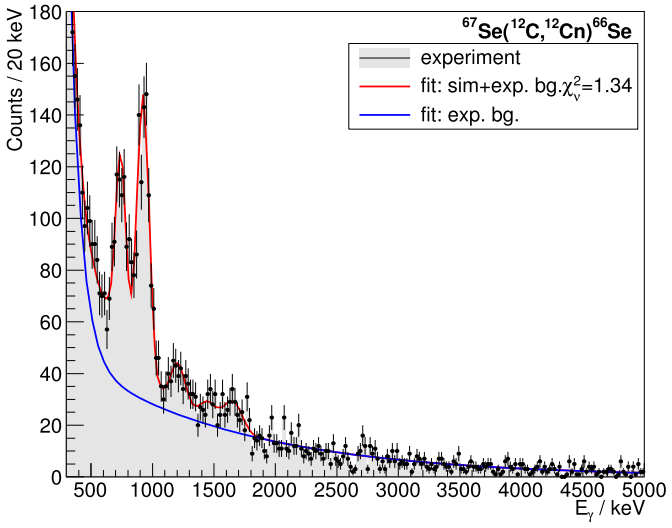

Fig. 1. Doppler-corrected singles γ-ray spectrum for ^{66}Se using addback procedure for the ^{67}Se(^{12}C,X)^{66}Se reaction channel. The data with error bars and shaded area represent the experimental spectrum, the red line is the simulation plus a double-exponential background, and the latter function (exponential background) is also plotted separately as a blue line.

Table 1
Properties of γ rays determined by fitting the singles spectrum of the ^{67}Se(^{12}C,X)^{66}Se reaction channel. E_γ is the energy, I_γ is the relative intensity, C is the statistical confidence, and σ_γ is the γ-ray-production cross section.

E_γ (keV)	I_γ	C	σ_γ (mb)
744(6)	50(5)	11.0σ	2.09(19)
927(4)	100	20.7σ	4.19(26)
1210(17)	20(4)	4.6σ	0.85(17)
1460(32)	10(4)	3.3σ	0.41(16)
1661(23)	21(4)	4.3σ	0.87(17)

of 1000-2000 keV. The statistical confidence, the energy, and the intensity of these peaks were deduced by using our Geant4 application which could provide the response function of the CATANA array for a γ ray emitted by the fast-moving projectile taking into account the intrinsic experimental resolution of the CsI(Na) crystals. The resulting response functions were added together with individual scaling parameters plus the double-exponential background function to fit the spectrum using the likelihood method [36] of the ROOT framework [37], which gives more reliable results for fitting spectra with low statistics [38,32]. The total fit with a reduced χ^2 (χ^2_ν) of 1.34 is presented by a red line in Fig. 1 while the background is shown by the blue line. Table 1 lists the properties of the observed five γ rays. The quoted uncertainties for the energy of the γ rays originated from the statistics, the energy calibration (4 keV), and the background estimation. The statistical confidence of the peaks was also checked with bin sizes of 25 keV and 40 keV, and proved to stay above the 3σ limit of unambiguous existence. Two of the transitions at 927 keV and at 1460 keV correspond to the transition reported at 929(7) keV and 929(2) keV and at 1456(2) keV in previous works [16,17].

The statistics also allowed us to prepare a $\gamma\gamma$ matrix with a multiplicity of 2 for the CATANA array to discover the relation between the γ rays. The coincidence spectra are plotted in Fig. 2 where the grey shaded spectra result from the coincidence with a γ ray of the indicated energy and the blue (background) spectra from a gate just displaced in energy from the energy of that γ ray. The panels A, B, and C show that the transitions at 744 keV, 1210 keV, and 1460 keV are in coincidence with the one at 927 keV. Owing to the reduction of the background in the coincidence spectra, the plot for the low-energy events in coincidence with the 927-keV transition (shown in panel D), indicates an additional transition at 299(31) keV. Due to the low statistics, the existence of this peak is questionable, however, it is in accordance with the simulated response of the CATANA array plotted by the red line. This transition might correspond to the one at 273(5) keV proposed earlier based on the singles spectrum of the two-neutron removal channel [16] but could not, in this previous study, be confirmed as a transition in ^{66}Se.

4. Discussion and interpretation of the results

In order to interpret the observed data a shell-model calculation was performed using JUN45 interaction which was developed to describe spectroscopy of nuclei comprised in the $pf_{5/2}g_{9/2}$ valence space [39]. We note that the same interaction was also used in the earlier study of ^{66}Se [16] although with a few modifications to account for the mirror energy differences. The shell-model codes ANTOINE and NATHAN [40,41] were employed to obtain the energy spectra, spectroscopic factors and electromagnetic transition rates. As recommended in the original publication for the JUN45 interaction [39], we used effective charges of $e_p = 1.5e$ and $e_n = 1.1e$ to evaluate the $E2$ transitions.

The calculated level scheme, the γ-ray branching ratios and the spectroscopic factors are plotted in Fig. 3 denoted as "shell model" together with the information from the mirror nucleus ^{66}Ge. The proton separation energy (S_p) is not known for ^{66}Se but the mass systematics suggests a value of 2.01(22) MeV [42]. Therefore the levels are shown up to 2.5 MeV since we do not expect to observe higher-lying states by γ-ray spectroscopy. The experimental 927-keV transition was proposed to connect the 2^+_1 state and the ground state earlier [16,17], which is also supported by the facts that it is the strongest transition in our singles spectrum and close in energy to the value for same state in the mirror nucleus. The observed 744-keV transition was found to be in coincidence with the 927-keV transition, which establishes a state at 1671 keV. This state is feasibly connected to the ground state by the experimental 1661(23)-keV transition because it is not in coincidence with the 927-keV transition. Furthermore, this state is a good candidate for the 2^+_2 state because its energy and decay pattern are close to that of the 2^+_2 state in the mirror nucleus. This assignment is supported by the fact that the first excited state in the shell-model calculation with relatively large spectroscopic factor is the 2^+_2, and the calculated branching ratios resemble the experimental ones. The observed 1210-keV and the 1460-keV transitions, being coincident with the 927-keV transition, places levels at 2137-keV and 2387-keV, respectively. The counterparts of these states in the shell model are likely the 2^+_3 and the 2^+_4 states due to their high calculated spectroscopic factors. The 299-keV transition observed only in the spectrum coincident with the 927-keV transition can be tentatively placed to connect the 0^+_2 and the 2^+_1 levels, as was hypothesized earlier [16].

Such a low-lying excited 0^+ state suggests shape coexistence in the nucleus. The intrinsic shape associated to the calculated shell-model states can be estimated from the $E2$ matrix elements following the same method which is applied in multipole Coulomb excitation formalism. The model-independent n-body quadrupole moments introduced in Ref. [43] were thus calculated to extract β_2 and γ parameters. The β_2 deformation deduced from the 2-body moments is similar for both 0^+ states: 0.26 and 0.27, respectively. The nucleus, however, appears to be non-axial with $\gamma = 31^\circ$ in the ground state and $\gamma = 22^\circ$ in the 0^+_2 state. More interestingly, the 3-body moments have opposite signs, which results in intrinsic quadrupole moments corresponding to an oblate ground state and prolate 0^+_2 state.

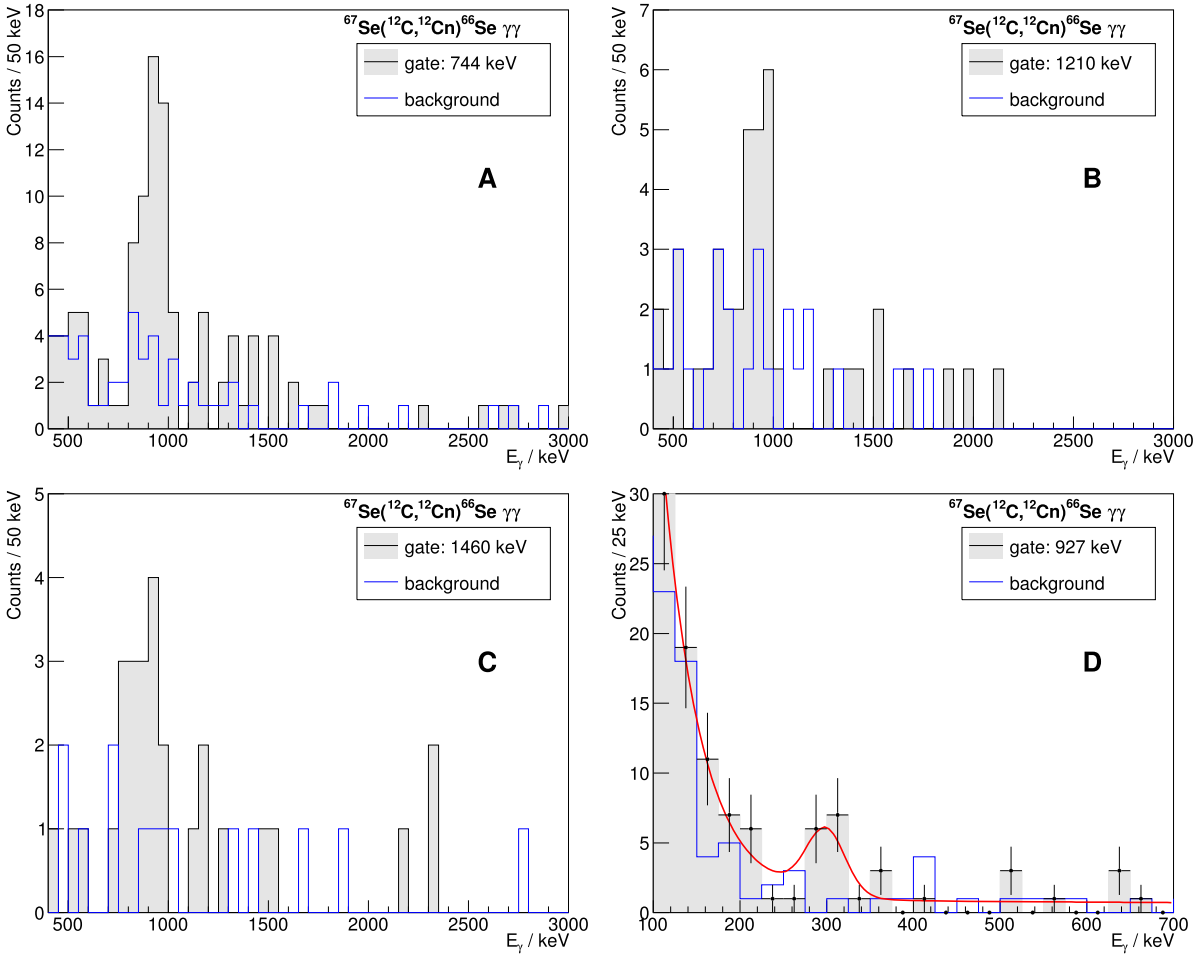

Fig. 2. Doppler-corrected coincidence γ-ray spectra for ^{66}Se using addback procedure for the ^{67}Se(^{12}C,X)^{66}Se reaction channel. The data with a grey shaded area represent the experimental spectrum by selecting events in the $\gamma\gamma$ matrices in coincidence with a prompt γ ray, while the blue background spectrum was created by selecting a gate right beside the prompt γ ray in question. A: events coincident with the 744-keV transition, B: events coincident with the 1210-keV transition, C: events coincident with the 1460-keV transition, D: low-energy events coincident with the 927-keV transition; the red line is the simulation plus a double-exponential background.

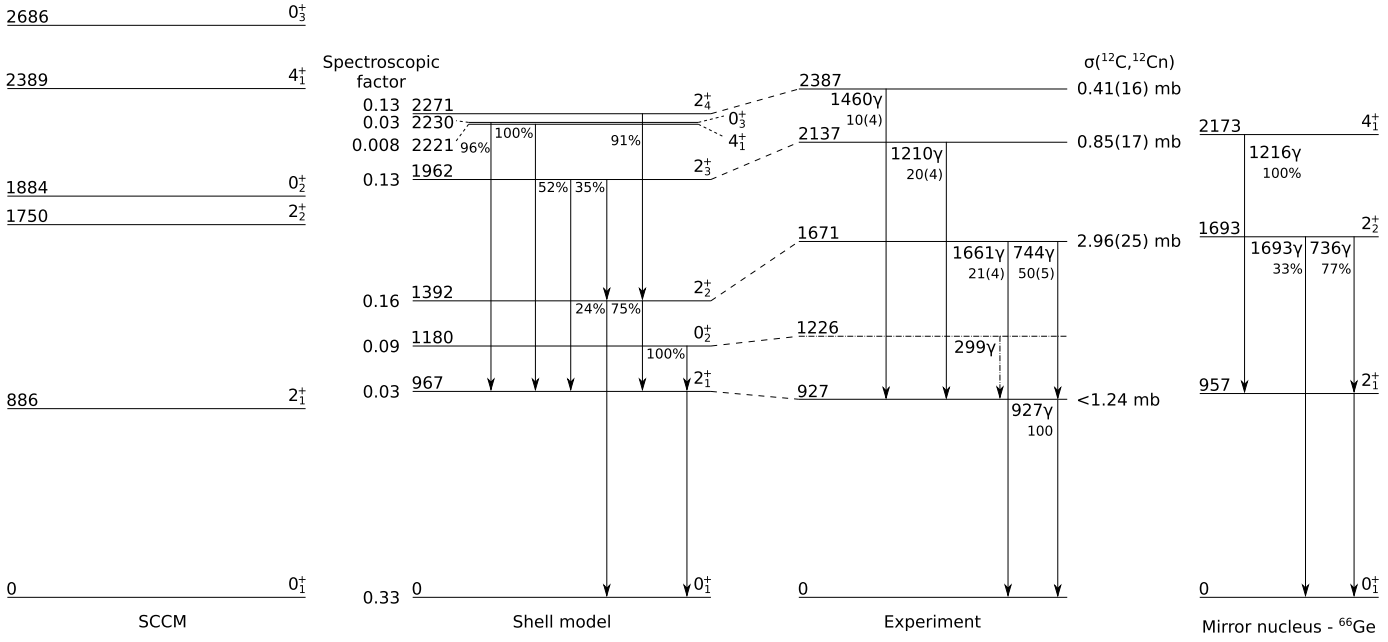

Fig. 3. The ^{66}Se level schemes, below the proton separation energy of 2.01(22) MeV [42], from the symmetry conserving configuration mixing model (SCCM), shell model, the present data, as well as that for the mirror nucleus are shown.

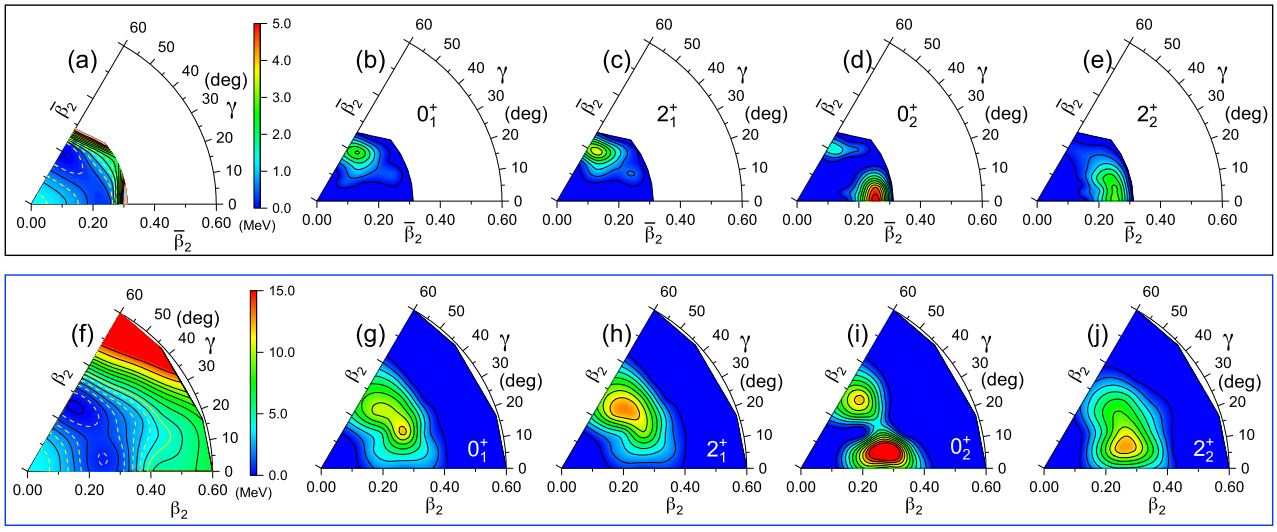

Fig. 4. The particle-number projected energy surface with JUN45 interaction (a) and Gogny D1S energy density functional (f). (b-c): Collective wave functions for the lowest states of the ground state band with JUN45 interaction. (d-e): Collective wave functions for the lowest states of the ground state band with Gogny D1S energy density functional. (g-h): Collective wave functions for the lowest states of the first excited band with JUN45 interaction. (i-j): Collective wave functions for the lowest states of the first excited state band with Gogny D1S energy density functional.

To get further insight into intrinsic shapes of ^{66}Se, calculations were performed with the projected generator coordinate method (PGCM) using the same interaction and valence space (JUN45) using the suite TAURUS [44,45]. Such a method aims at obtaining variational approximations to the exact wave functions. Its practical implementation can be divided in three steps: (a) the definition of a set of Hartree-Fock-Bogolyubov (HFB) intrinsic states; (b) the symmetry restoration by particle-number and angular-momentum projection of such HFB states; and, (c) the linear combination of the projected-HFB states to obtain the final results. In the present case, the intrinsic HFB states were obtained by minimizing the particle-number projected (PNP) energy for different values of the quadrupole deformation parameters, β_2. Because JUN45 interaction is defined in a restricted valence space with a core, the deformations that could be attained within this model was limited. In addition, bare quadrupole operators were multiplied by a factor of 2.6 to account for the particles in the core through an "effective mass", producing an effective deformation parameter $\overline{\beta}_2$. This factor was chosen to be compatible with the effective charges used in the evaluation of electromagnetic properties [46]. A first interpretation of the collective character of the nucleus was obtained with the PNP energy surface shown in Fig. 4(a). Here, two minima at $(\overline{\beta}_2, \gamma) = (0.26, 60°)$ (oblate) and $(0.22, 0°)$ (prolate) connected by a rather flat energy in the γ direction were obtained. Therefore, both shape coexistence and shape mixing could be relevant in the description of the states of ^{66}Se with JUN45. The resulting PGCM spectrum (not shown) were very similar to the exact result labeled as "shell model" in Fig. 3. The collective wave functions (c.w.f.'s) for the lowest states of the ground-state (first-excited) band, built on top of the $0_1^+(0_2^+)$ state are plotted in Fig. 4(b)-(c) (Fig. 4(d)-(e)). These c.w.f.'s represent the weights of the different intrinsic deformations in the construction of each individual state. Hence, the states in the ground state band are built with oblate configurations located on top of the energy well found in the PNP energy surface. On the other hand, the 0_2^+ state shows shape mixing. Hence, its c.w.f. has a main peak around the prolate minimum obtained in the energy surface, and a smaller peak around the oblate deformations where the maximum of the ground-state c.w.f. is found. The c.w.f. of the 2_2^+ state also has its maximum at a prolate deformation with some extension towards the triaxial degree of freedom. The PGCM analysis predicts slightly smaller and less triaxial deformations than the values deduced with the method of Ref. [43] but the overall behavior is consistent with those values. These results indicate that the nucleus ^{66}Se computed with JUN45 shows a shape coexistent pattern with two distinctive configurations, an oblate ground state and a mostly prolate (and slightly more deformed) excited configurations.

Finally, we also performed PGCM calculations of the same kind as those described above but with the Gogny D1S energy density functional (EDF). This implementation is also known as symmetry conserving configuration mixing (SCCM) method [47,48]. In this case, since they are no-core calculations, no effective quadrupole operators were needed to define $(\overline{\beta}_2, \gamma)$ and the nucleus could be deformed with almost no restrictions. The PNP energy surface, $0_1^+, 2_1^+, 0_2^+$ and 2_2^+ c.w.f.'s are represented in Fig. 4(f)-(j), respectively. The EDF energy surface also shows two minima at $\beta_2 = 0.3$, one more oblate and another more prolate, that are connected through the triaxial degree of freedom. After symmetry restoration and configuration mixing, the ground state c.w.f. shows a noticeable shape mixing from $\gamma = 10°$ to $60°$ at $\beta_2 \approx 0.3$. The 2_1^+ state also presents such a mixing but the peak is shifted from $\gamma = 20°$ towards 45°. Similar to the JUN45 case, the 0_2^+ c.w.f. shows two maxima at the position of the two energy wells, being the more prolate one the larger, and the 0_2^+ c.w.f. is extended in the γ direction from its maximum at a more prolate configuration. Hence, Gogny-SCCM calculations also predict two distinctive structures at low excitation energy but with larger mixing along the γ degree of freedom, and slightly larger intrinsic deformation. The energy spectrum obtained with the present Gogny EDF is labeled as "SCCM" in Fig. 3 where the 2_1^+ excitation energy is in good agreement with both the experimental value and the JUN45 calculations but the 2_2^+ state is below the 0_2^+, contrary to shell model calculations. Previous calculations using the five-dimensional collective Hamiltonian with Gogny D1S also showed this inversion of the states [16] although in the present SCCM implementation these two levels are very close in energy. Nevertheless, both SCCM calculations predict large overlaps between the 0_2^+ and the 2_2^+ collective wave functions that produce large $B(E2, 2_2^+ \rightarrow 0_2^+)$ values, namely, 324 e^2fm^4 and 227 e^2fm^4 for Gogny D1S and JUN45 (with 1.5 and 0.5 proton and neutron effective charges), respectively.

5. Summary

The low-lying bound excited states of ^{66}Se were investigated by the neutron knock-out reaction using a thin ^{12}C target. Four new and two known transitions were observed. Using their energy and coincidence relations compared to our shell-model calculation based on the JUN45 interaction and the mirror nucleus ^{66}Ge, the level scheme was successfully constructed. The 2_2^+ state was unambiguously identified and the 0_2^+ state was also tentatively placed in the level scheme. These states belong to the same band according to our SCCM calculations which, in accordance with the shell model, predict coexisting triaxial-deformed configurations (more oblate in the ground state band and more prolate in the first excited state band).

Declaration of competing interest

The authors declare that they have no known competing financial interests or personal relationships that could have appeared to influence the work reported in this paper.

Data availability

Data will be made available on request.

Acknowledgements

Z. E, Cs. D., Z. H., Gy. H., I. K., L. S. and M. M. J. were supported by NKFIH under projects TKP2021-NKTA-42, K128947, 2021-4.1.2-NEMZ_KI-2021-00005 and NN128072. T. R. R. acknowledges funding from the Spanish MICINN under contract PID2021-127890NB-I00 and support from GSI-Darmstadt computing facilities. Y. T. was supported by JSPS Grant-in-Aid for Scientific Research Grants No. JP21H01114. K. J. C. acknowledges the JSPS International Fellowship for Research in Japan, hosted by the Tokyo Institute of Technology. D. S. A., K. I. H. and D. K. acknowledge the support from the IBS grant funded by the Korea government (No. IBS-R031-D1). V. P. acknowledges the KAKENHI Grant-in-Aid for Young Scientists B No. 16K17719. A. A. acknowledges the JSPS International Fellowships for their travel support.

References

[1] A. Poves, J. Phys. G, Nucl. Part. Phys. 43 (2016) 020401.
[2] H. Morinaga, Phys. Rev. 101 (1956) 254.
[3] K. Heyde, J.L. Wood, Rev. Mod. Phys. 83 (2011) 1467.
[4] P.E. Garrett, M. Zielińska, E. Clément, Prog. Part. Nucl. Phys. 124 (2022) 103931.
[5] D. Abriola, A. Sonzogni, Nucl. Data Sheets 111 (2010) 1.
[6] A. Mukherjee, S. Bhattacharya, T. Trivedi, R.P. Singh, S. Muralithar, D. Negi, R. Palit, S. Nag, S. Rajbanshi, M.K. Raju, et al., Phys. Rev. C 105 (2022) 014322.
[7] B. Singh, A.R. Farhan, Nucl. Data Sheets 107 (2006) 1923.
[8] E.A. McCutchan, C.J. Lister, T. Ahn, V. Anagnostatou, N. Cooper, M. Elvers, P. Goddard, A. Heinz, G. Ilie, D. Radeck, et al., Phys. Rev. C 87 (2013) 014307.
[9] B. Singh, Nucl. Data Sheets 74 (1995) 63.
[10] G. Gürdal, E. McCutchan, Nucl. Data Sheets 136 (2016) 1.
[11] S. Mukhopadhyay, B.P. Crider, B.A. Brown, A. Chakraborty, A. Kumar, M.T. McEllistrem, E.E. Peters, F.M. Prados-Estévez, S.W. Yates, Phys. Rev. C 99 (2019) 014313.
[12] E.A. McCutchan, C.J. Lister, T. Ahn, R.J. Casperson, A. Heinz, G. Ilie, J. Qian, E. Williams, R. Winkler, V. Werner, Phys. Rev. C 83 (2011) 024310.
[13] J. Ljungvall, A. Görgen, M. Girod, J.-P. Delaroche, A. Dewald, C. Dossat, E. Farnea, W. Korten, B. Melon, R. Menegazzo, et al., Phys. Rev. Lett. 100 (2008) 102502.
[14] G. Rainovski, H. Schnare, R. Schwengner, C. Plettner, L. Käubler, F. Dönau, I. Ragnarsson, J. Eberth, T. Steinhardt, O. Thelen, et al., J. Phys. G, Nucl. Part. Phys. 28 (2002) 2617.
[15] K. Wimmer, W. Korten, P. Doornenbal, T. Arici, P. Aguilera, A. Algora, T. Ando, H. Baba, B. Blank, A. Boso, et al., Phys. Rev. Lett. 126 (2021) 072501.
[16] A. Obertelli, T. Baugher, D. Bazin, S. Boissinot, J.-P. Delaroche, A. Dijon, F. Flavigny, A. Gade, M. Girod, T. Glasmacher, et al., Phys. Lett. B 701 (2011) 417.
[17] P. Ruotsalainen, D.G. Jenkins, M.A. Bentley, R. Wadsworth, C. Scholey, K. Auranen, P.J. Davies, T. Grahn, P.T. Greenlees, J. Henderson, et al., Phys. Rev. C 88 (2013) 041308.
[18] T. Kubo, D. Kameda, H. Suzuki, N. Fukuda, H. Takeda, Y. Yanagisawa, M. Ohtake, K. Kusaka, K. Yoshida, N. Inabe, et al., Prog. Theor. Exp. Phys. 2012 (2012) 03C003.
[19] N. Fukuda, T. Kubo, T. Ohnishi, N. Inabe, H. Takeda, D. Kameda, H. Suzuki, Nucl. Instrum. Methods Phys. Res., Sect. B, Beam Interact. Mater. Atoms 317 (2013) 323.
[20] T. Kubo, in: 14th International Conference on Electromagnetic Isotope Separators and Techniques Related to Their Applications, Nucl. Instrum. Methods Phys. Res., Sect. B, Beam Interact. Mater. Atoms 204 (2003) 97.
[21] K. Kimura, T. Izumikawa, R. Koyama, T. Ohnishi, T. Ohtsubo, A. Ozawa, W. Shinozaki, T. Suzuki, M. Takahashi, I. Tanihata, et al., Nucl. Instrum. Methods Phys. Res., Sect. A, Accel. Spectrom. Detect. Assoc. Equip. 538 (2005) 608.
[22] H. Kumagai, A. Ozawa, N. Fukuda, K. Sümmerer, I. Tanihata, Nucl. Instrum. Methods Phys. Res., Sect. A, Accel. Spectrom. Detect. Assoc. Equip. 470 (2001) 562.
[23] H. Kumagai, T. Ohnishi, N. Fukuda, H. Takeda, D. Kameda, N. Inabe, K. Yoshida, T. Kubo, Nucl. Instrum. Methods Phys. Res., Sect. B, Beam Interact. Mater. Atoms 317 (2013) 717.
[24] Y. Togano, T. Nakamura, Y. Kondo, M. Shikata, T. Ozaki, A. Saito, T. Tomai, M. Yasuda, H. Yamada, N. Chiga, et al., Nucl. Instrum. Methods Phys. Res., Sect. B, Beam Interact. Mater. Atoms 463 (2020) 195.
[25] T. Kobayashi, N. Chiga, T. Isobe, Y. Kondo, T. Kubo, K. Kusaka, T. Motobayashi, T. Nakamura, J. Ohnishi, H. Okuno, et al., in: XVIth International Conference on ElectroMagnetic Isotope Separators and Techniques Related to Their Applications, December 2-7, 2012 at Matsue, Japan, Nucl. Instrum. Methods Phys. Res., Sect. B, Beam Interact. Mater. Atoms 317 (2013) 294.
[26] ROOT MultiDimFit, https://root.cern.ch/doc/master/classTMultiDimFit.html. (Accessed 1 April 2022).
[27] V. Panin, M. Kurokawa, K. Yoneda, H. Baba, J.C. Blackmon, Z. Elekes, Z. Halász, D.H. Kim, T. Motobayashi, H. Otsu, et al., RIKEN Accel. Prog. Rep. 49 (2016) 164.
[28] V. Panin, Z. Elekes, Z. Halász, G. Hegyesi, C. Dósa, L. Trache, A. Chilug, I. Stefanescu, D. Tudor, M. Sasano, et al., RIKEN Accel. Prog. Rep. 51 (2018) 148.
[29] A.I. Stefanescu, V. Panin, L. Trache, T. Motobayashi, H. Otsu, A. Saastamoinen, T. Uesaka, L. Stuhl, J. Tanaka, D. Tudor, et al., Eur. Phys. J. A 58 (2022) 223.
[30] P. Doornenbal, Prog. Theor. Exp. Phys. 2012 (2012) 03C004.
[31] M.L. Cortés, P. Doornenbal, M. Dupuis, S.M. Lenzi, F. Nowacki, A. Obertelli, S. Péru, N. Pietralla, V. Werner, K. Wimmer, et al., Phys. Rev. C 97 (2018) 044315.
[32] H.N. Liu, A. Obertelli, P. Doornenbal, C.A. Bertulani, G. Hagen, J.D. Holt, G.R. Jansen, T.D. Morris, A. Schwenk, R. Stroberg, et al., Phys. Rev. Lett. 122 (2019) 072502.
[33] Y. Sun, A. Obertelli, P. Doornenbal, C. Barbieri, Y. Chazono, T. Duguet, H. Liu, P. Navrátil, F. Nowacki, K. Ogata, et al., Phys. Lett. B (ISSN 0370-2693) 802 (2020) 135215.
[34] M. Cortés, W. Rodriguez, P. Doornenbal, A. Obertelli, J. Holt, S. Lenzi, J. Menéndez, F. Nowacki, K. Ogata, A. Poves, et al., Phys. Lett. B 800 (2020) 135071.
[35] M.L. Cortés, W. Rodriguez, P. Doornenbal, A. Obertelli, J.D. Holt, J. Menéndez, K. Ogata, A. Schwenk, N. Shimizu, J. Simonis, et al., Phys. Rev. C 102 (2020) 064320.
[36] S. Baker, R.D. Cousins, Nucl. Instrum. Methods Phys. Res. 221 (1984) 437.
[37] I. Antcheva, M. Ballintijn, B. Bellenot, M. Biskup, R. Brun, N. Buncic, P. Canal, D. Casadei, O. Couet, V. Fine, et al., Comput. Phys. Commun. 180 (2009) 2499.
[38] Nuclear structure in the vicinity of ^{78}Ni: in-beam gamma-ray spectroscopy of ^{79}Cu through proton knockout, https://tel.archives-ouvertes.fr/tel-01637435/document. (Accessed 10 April 2022).
[39] M. Honma, T. Otsuka, T. Mizusaki, M. Hjorth-Jensen, Phys. Rev. C 80 (2009) 064323.
[40] E. Caurier, F. Nowacki, Acta Phys. Pol. B 30 (1999) 705.
[41] E. Caurier, G. Martínez-Pinedo, F. Nowacki, A. Poves, A.P. Zuker, Rev. Mod. Phys. 77 (2005) 427.
[42] M. Wang, W. Huang, F. Kondev, G. Audi, S. Naimi, Chin. Phys. C 45 (2021) 030003.
[43] K. Kumar, Phys. Rev. Lett. 28 (1972) 249.
[44] B. Bally, A. Sánchez-Fernández, T.R. Rodríguez, Phys. Rev. C 100 (2019) 044308.
[45] A. Sánchez-Fernández, B. Bally, T.R. Rodríguez, Phys. Rev. C 104 (2021) 054306.
[46] D.D. Dao, F. Nowacki, Phys. Rev. C 105 (2022) 054314.
[47] T.R. Rodríguez, J.L. Egido, Phys. Rev. C 81 (2010) 064323.
[48] L.M. Robledo, T.R. Rodríguez, R.R. Rodríguez-Guzmán, J. Phys. G, Nucl. Part. Phys. 46 (2018) 013001.